HHS Public Access

Author manuscript

Arterioscler Thromb Vasc Biol. Author manuscript; available in PMC 2023 September 01.

Published in final edited form as:

Arterioscler Thromb Vasc Biol. 2022 September ; 42(9): 1139–1151. doi:10.1161/ATVBAHA.121.317156.

ILRUN Promotes Atherosclerosis through Lipid-dependent and Lipid-independent Factors

Xin Bi[1,3,*], **Sylvia Stankov**[1], **Paul C. Lee**[1], **Ziyi Wang**[5], **Xun Wu**[5], **Li Li**[2], **Yi-An Ko**[1], **Lan Cheng**[2], **Hanrui Zhang**[5], **Nicholas J. Hand**[3], **Daniel J. Rader**[1,3,4,*]

[1]Division of Translational Medicine and Human Genetics, Department of Medicine, Perelman School of Medicine, University of Pennsylvania, Philadelphia, PA, USA

[2]Cardiovascular Institute, Perelman School of Medicine, University of Pennsylvania, Philadelphia, PA, USA

[3]Department of Genetics, Perelman School of Medicine, University of Pennsylvania, Philadelphia, PA, USA

[4]Department of Pediatrics, Perelman School of Medicine, University of Pennsylvania, Philadelphia, PA, USA

[5]Cardiometabolic Genomics Program, Division of Cardiology, Department of Medicine, Columbia University Irving Medical Center, New York, NY, USA

Abstract

Background: Common genetic variation in close proximity to the *ILRUN* gene are significantly associated with coronary artery disease (CAD) as well as with plasma lipid traits. We recently demonstrated that hepatic ILRUN regulates lipoprotein metabolism *in vivo* in mice. However, whether ILRUN, which is expressed in vascular cells, directly impacts atherogenesis remains unclear. We sought to determine the role of ILRUN in atherosclerosis development in mice.

Methods: For our study we generated global *Ilrun* deficient (*Ilrun*KO) male and female mice on two hyperlipidemic backgrounds: low density lipoprotein receptor knockout (*Ldlr*KO) and apolipoprotein E knockout (*Apoe*KO) (double KO, DKO).

Results: Compared with littermate control mice (single *Ldlr*KO or *Apoe*KO), deletion of *Ilrun* in DKO mice resulted in significantly attenuated both early and advanced atherosclerotic lesion development, as well as reduced necrotic area. DKO mice also had significantly decreased plasma cholesterol levels, primarily attributable to non-HDL cholesterol. Hepatic-specific reconstitution of *ILRUN* in DKO mice on the *Apoe*KO background normalized plasma lipids, but atherosclerotic lesion area and necrotic area remained reduced in DKO mice. Further analysis showed that loss

[*]Address correspondence to: Daniel J. Rader, MD, University of Pennsylvania, 11-125 Smilow Center for Translational Research, 3400 Civic Center Blvd, Philadelphia, PA, 19104-5158, rader@pennmedicine.upenn.edu; Xin Bi, MBBS, PhD, University of Pennsylvania, 11-165 Smilow Center for Translational Research, 3400 Civic Center Blvd, Philadelphia, PA, 19104-5158, xbi@pennmedicine.upenn.edu.

Disclosures

None

of *Ilrun* increased efferocytosis receptor MerTK expression in macrophages, enhanced *in vitro* efferocytosis, and significantly improved *in situ* efferocytosis in advanced lesions.

Conclusions: Our results support ILRUN as an important novel regulator of atherogenesis that promotes lesion progression and necrosis. It influences atherosclerosis through both plasma lipid-dependent and lipid-independent mechanisms. These findings support ILRUN as the likely causal gene responsible for genetic association of variants with CAD at this locus, and suggest that suppression of ILRUN activity might be expected to reduce atherosclerosis.

Graphical Abstract

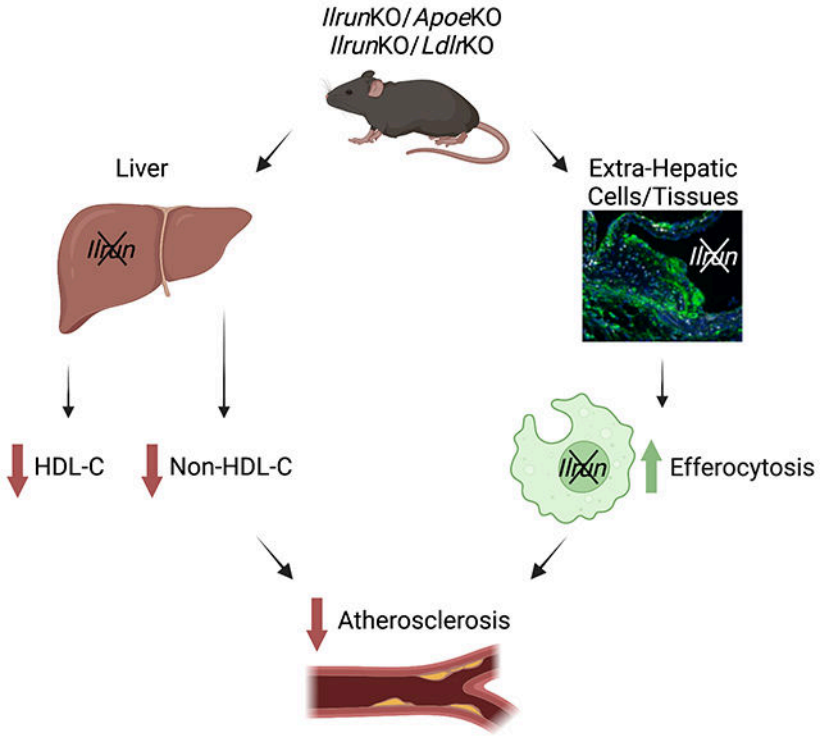

Keywords

lipoprotein metabolism; atherosclerosis; ILRUN

Introduction

Despite the widespread success of effective current therapies, atherosclerotic cardiovascular disease (ASCVD) remains a main leading cause of death globally[1], and represents an ongoing unmet medical need. Major efforts are ongoing to better understand the genetic architecture of ASCVD. To date, large-scale genome-wide association studies (GWAS) have discovered over 160 genomic loci that are significantly associated with coronary artery disease (CAD) risk[2]. One of these loci on chromosome 6 harbors the gene *ILRUN* (inflammation and lipid regulator with UBA-like and NBR1-like domains; previously *C6ORF106*). Variants at this same locus are also significantly associated with plasma LDL cholesterol (LDL-C) and HDL cholesterol (HDL-C)[3–6]. *ILRUN* is a recently characterized

and named gene that is ubiquitously expressed, including abundant expression in arterial tissues as well as in the liver[7]. It encodes a protein with two regions of sequence conservation: an N-terminal α-helical ubiquitin associated domain-like (UBA-like) domain and a "next to BRCA1 gene 1 protein-like" (NBR1-like) domain[8].

Prior research on ILRUN had mainly focused on the correlation of its expression in tumors with cancer prognosis[9–11]. While our knowledge of ILRUN remains limited, more recent studies in HeLa cells suggest a role for ILRUN in anti-viral immunity, where both conserved domains are necessary for ILRUN regulation of transcription factor IRF3 binding to DNA and downstream gene transcription[12,13]. Our previous work showed that hepatic ILRUN regulates plasma lipoprotein metabolism[14], consistent with the human genetic association with plasma lipid traits. We demonstrated that ILRUN promotes hepatic lipoprotein production *in vivo*, and that the UBA-like domain, but not the NBR-1 like domain, of ILRUN mediates its interaction with ubiquitinated proteins, including transcriptional regulators known to regulate lipid metabolic pathways. This interaction likely modulates target protein homeostasis and accessibility, thereby influencing lipoprotein metabolism at the level of gene transcription[14].

Given the human genetic association of the *ILRUN* locus to CAD[2,15,16] and the expression of ILRUN in arterial tissues[7] and vascular cells such as endothelial cells[17,18], we sought to investigate the relationship between ILRUN and atherosclerosis development in mice. We show that *Ilrun* deficiency markedly protected against atherogenesis in both the low-density lipoprotein receptor knockout (*Ldlr*KO) and apolipoprotein E knockout (*Apoe*KO) disease models. While *Ilrun* deficiency also reduced plasma cholesterol and non-HDL-C levels, normalization of plasma cholesterol by reconstitution of *ILRUN* in the liver failed to normalize the atherosclerosis phenotype. We found that *Ilrun* deficient mice and macrophages have enhanced *in situ* efferocytosis markers and *in vitro* efferocytosis respectively, which may contribute to the observed reduced atherosclerosis. These results establish ILRUN as a pro-atherogenic protein that acts through effects on plasma lipids as well as non-lipid-dependent mechanisms.

Methods

A detailed Methods section is available in Supplemental Material. All animal experiment protocols and procedures were reviewed and approved by the Institutional Animal Care and Use Committees of the University of Pennsylvania.

Data Availability

The majority of supporting data are presented within this article and its data supplement. Data that are not directly available are available from the corresponding author upon reasonable request.

Results

Genetic variations near *ILRUN* associated with CAD risk are associated with *ILRUN* expression in arterial tissues

The minor allele of a common *ILRUN* intronic SNP (rs2814993-A) is genome-wide significantly associated with *increased* CAD risk[2]. Phenome-wide association studies using the UK biobank data further confirmed the associations of rs2814993-A with increased risk of coronary atherosclerosis and ischemic heart disease, in addition to the most significant associations with hypertension and essential hypertension[30,31]. Human *ILRUN* is highly expressed in atherosclerosis-relevant tissues and cells, including aorta, tibial artery, coronary artery, and blood cells[7]. In analyses of human arterial tissue and blood gene expression data, we found that rs2814993-A is significantly associated with *increased* expression of *ILRUN* (Figure 1A), consistent with a model in which increased *ILRUN* expression leads to increased risk of CAD.

Ilrun is expressed in normal and atherosclerotic arteries in mice

We previously showed abundant *Ilrun* expression in normal aortas of C57BL/6 mice[14]. Our mouse model has lacZ knocked into the *Ilrun* locus, allowing for convenient evaluation of gene expression. Detailed histological analysis of normal and atherosclerotic mouse vascular tissues stained with X-gal confirmed expression in the vasculature, including brachiocephalic artery and thoracic aorta. Positive stains were consistent with expression in smooth muscle cells (SMC) and endothelial cells (EC) (Figure 1B). Indeed, immunohistochemistry with the SMC marker SM22α revealed a significant overlap between X-gal positive signals and SM22α positive stains in the normal vessel wall (Figure 1C). Publicly available data support *ILRUN* expression in human atherosclerotic plaques[32,33]. In our analysis of aortic root lesions in mice, ILRUN was present with positive stains colocalizing with SM22α+ SMC and Mac3+ macrophages (Figure 1D–F). Further analysis of a single cell RNA-seq dataset[27] of CD45+ leukocytes from the aortas of male *Ldlr*KO mice fed a high-fat diet for 11 weeks showed that *Ilrun* was highly expressed in myeloid cells, including monocytes and macrophages, as well as some dendritic cells, yet relatively lowly expressed in other immune cells (Figure S1). In short, *Ilrun* is ubiquitously expressed in both normal and atherosclerotic arteries in mice.

Global *Ilrun* deletion in *Ldlr*KO and *Apoe*KO mice attenuates atherogenesis

To evaluate atherosclerotic lesion development, we crossed *Ilrun*KO mice onto both the *Ldlr* and *Apoe*KO backgrounds. To investigate the impact of *Ilrun* on atherosclerosis development in a stage-specific manner (i.e., both early and advanced lesions), *Ilrun*KO/*Ldlr*KO and littermate control *Ldlr*KO mice were maintained on a normal laboratory diet (ND) for 24 weeks or switched from ND to a western type diet (WTD) for 16 weeks. In male *Ldlr*KO mice fed a ND, we detected only small early-stage lesions. Loss of *Ilrun* resulted in a significant ~67% decrease in average lesion area (Figure 2A). As expected, male mice challenged with WTD for 16 weeks developed more advanced lesions that were significantly smaller (~50% decrease) in *Ilrun*KO/*Ldlr*KO mice compared with *Ldlr*KO control mice (Figure 2B). Similarly, female *Ilrun*KO/*Ldlr*KO mice on WTD displayed a significant ~66% reduction in lesion size relative to *Ldlr*KO controls (Figure S2A). These

results on the *Ldlr* deficient genetic background support an atherogenic role for *Ilrun* in both early and advanced lesion development.

Atherosclerotic lesion progression was also assessed in *Apoe*KO mice. *Ilrun*KO/*Apoe*KO and littermate control *Apoe*KO mice were either maintained on ND for 28 weeks or fed with WTD for 10 weeks, to accelerate atherogenesis. The absence of *Ilrun* resulted in markedly smaller lesion areas in male mice fed either ND (~60% reduced) or WTD (~50% reduced) (Figure 2C–D). *Ilrun* deficiency also protected female *Apoe*KO mice against atherogenesis; lesion areas were decreased significantly, ~80% on ND and over 30% that did not reach statistical significance on WTD in *Ilrun*KO/*Apoe*KO vs. *Apoe*KO mice (Figure S2B–C). Along with findings from *Ldlr*KO mice, these data unequivocally demonstrate an atherogenic role for *Ilrun* that is evident for both sexes of mice and independent of the disease model.

Ilrun deficiency reduces plasma lipid levels in *Ldlr*KO and *Apoe*KO mice

Plasma lipid levels of experimental mice during disease progression were monitored with periodic measurements. In ND-fed male *Ldlr*KO mice at 24 weeks of age, we observed significantly lower plasma total cholesterol (TC) in *Ilrun*KO/*Ldlr*KO vs. *Ldlr*KO mice (Figure 3A), which was attributed to lower high-density lipoprotein cholesterol (HDL-C) and non-HDL-C levels (Figure 3B–C). Fast protein liquid chromatography (FPLC) analysis revealed a predominant reduction of cholesterol mass associated with LDL particles in *Ilrun*KO/*Ldlr*KO relative to control *Ldlr*KO mice (Figure 3D). Similarly, compared to control *Ldlr*KO mice, ND-fed *Ilrun*KO/*Ldlr*KO had significantly lower plasma phospholipids (PL) and triglyceride (TG) levels (Figure S3A–B), primarily in fractions in the VLDL range. In male mice fed WTD, the increase in cholesterol in *Ilrun*KO/*Ldlr*KO mice was significantly attenuated relative to the *Ldlr*KO mice throughout the study (Figure 3E–G and S3D–E). The lower plasma TC and TG in *Ilrun*KO/*Ldlr*KO mice were mainly due to effects on non-HDL particles (Figure 3H and S3F). Female *Ilrun*KO/*Ldlr*KO vs. control mice displayed a similar pattern of lower plasma lipids (Figure S3G–K). These data show that the lipid-regulatory effect of *Ilrun* is independent of the *Ldlr*, consistent with a model that *Ilrun* deficiency lowers non-HDL-C by reducing lipoprotein production.

We also investigated whether *Ilrun* regulates lipid metabolism similarly in *Apoe*KO mice. In ND-fed male mice, plasma TC was significantly lower (over 30%) in *Ilrun*KO/*Apoe*KO relative to *Apoe*KO mice (Figure 3I). This difference was primarily driven by markedly lower non-HDL-C levels (Figure 3J–K), in particular cholesterol associated with VLDL particles (Figure 3L). Additionally, plasma PL was also significantly lower in mice lacking *Ilrun* whereas comparable TG was observed between genotypes (Figure S4A–C). While WTD consumption greatly induced plasma lipid levels in both groups, male *Ilrun*KO/*Apoe*KO mice exhibited an attenuated response to WTD leading to noticeably lower plasma TC, HDL-C, non-HDL-C, especially VLDL-C, and PL levels throughout the course of disease progression (Figure 3M–P and S4D). Plasma TG did not differ significantly between genotypes over the course of study (Figure S4E–F). Lack of *Ilrun* in female *Apoe*KO mice resulted in significantly lower plasma TC and non-HDL-C levels on both ND and WTD. However, unlike male mice, plasma TG on WTD, HDL-C, and PL levels on both ND and

WTD-fed female mice were minimally impacted by the absence of *Ilrun.* Plasma TG in ND-fed female *Ilrun*KO/*Apoe*KO mice was instead significantly higher relative to *Apoe*KO mice (Figure S4G–Q). Altogether, our results uncovered a predominant role for *Ilrun* in non-HDL-C metabolism in the face of hyperlipidemia due to *Apoe* deficiency.

Hepatic reconstitution of *ILRUN* normalizes plasma lipids in *Ilrun*KO mice but atherosclerosis remains reduced

We previously showed that *Ilrun* expression in hepatocytes is a primary mediator of plasma lipid regulation by *Ilrun* in mice wild-type for *Ldlr* and *Apoe*[14]. To test whether the altered plasma lipid profile during atherogenesis in mice globally deficient in *Ilrun* is also a result of loss of hepatic *Ilrun* expression, we used an adeno-associated virus (AAV) to drive human *ILRUN* expression specifically in the hepatocytes of *Ilrun*KO/*Apoe*KO mice. ND-fed male *Apoe*KO control and *Ilrun*KO/*Apoe*KO mice were injected with either an empty AAV8 vector (AAV-null) or an *ILRUN* expressing AAV8 vector (AAV-*ILRUN*). Two weeks after AAV injection, these mice were switched from ND to WTD for 10 weeks to further induce hyperlipidemia. As expected, WTD consumption robustly elevated plasma lipids for all study groups. Consistent with our observations in *Apoe*KO mice, *Ilrun*KO/*Apoe*KO vs. *Apoe*KO mice injected with AAV-null exhibited markedly lower plasma TC and non-HDL-C levels. In contrast, hepatic human *ILRUN* reconstitution in *Ilrun*KO/*Apoe*KO mice via AAV-*ILRUN* restored plasma cholesterol to those of *Apoe*KO-AAV-null control mice levels throughout the study (Figure 4A–C). These data support the notion that *Ilrun* expression in hepatocytes is primarily responsible for the altered plasma lipid profile seen in global *Ilrun* deficient mice under hyperlipidemic conditions.

To investigate whether *Ilrun* exacerbates atherogenesis solely by regulating atherogenic lipoprotein metabolism, we examined atherosclerosis development in mice from the AAV8 study that were globally *Ilrun* deficient, but with *ILRUN* expression solely in hepatocytes. This approach allowed us to minimize the differences in plasma lipids between genotypes and test for effects of *Ilrun* on atherogenesis that are independent of lipid levels. As previously noted, aortic root lesion area trended smaller (~55%) in AAV-null injected *IlrunKO*/*Apoe*KO mice compared to their *Apoe*KO counterparts (p=0.061). Intriguingly, despite the normalization of plasma cholesterol, a ~40% smaller average lesion size that did not reach statistical significance (p=0.075) was observed in AAV-*ILRUN* injected *IlrunKO*/*Apoe*KO mice relative to AAV-null injected *Apoe*KO mice (Figure 4D–E), suggesting that extra-hepatic *Ilrun* expression may contribute to atherogenesis by a lipid-independent mechanism.

Ilrun deficiency promotes *in situ* efferocytosis and reduces plaque necrosis

Analysis of transcriptomic data from laser micro-dissected macrophages from human carotid plaques[34] revealed that *ILRUN* expression was increased in cells from ruptured vs. stable plaques (Figure 5A). This suggests that ILRUN may affect plaque stability in humans. *Apoe*KO mice develop atherosclerotic lesions that are complex at later stages[35]. We evaluated lesion composition to gain insights into lipid-independent effects *Ilrun* may have on atherogenesis and markers of plaque stability. When acellular nonfibrotic lesion necrotic areas were quantitated in female mice with spontaneous lesion development,

lesional necrotic area was dramatically reduced (~ 70%) in *Ilrun*KO/*Apoe*KO vs. *Apoe*KO mice (Figure S5A). For male mice in the hepatic *ILRUN* reconstitution study, a consistent significant ~90% reduction in necrotic lesions was detected in AAV-null injected *Ilrun*KO/*Apoe*KO vs. *Apoe*KO mice, confirming a role for *Ilrun* in aggravating lesion necrosis. Importantly, normalization of plasma lipid profiles in *Ilrun* deficient mice failed to reverse the relative difference in necrosis between genotypes (Figure 5B–C), demonstrating that loss of extra-hepatic *Ilrun* contributes to atheroprotection independent of plasma lipids.

Total collagen content measured as a percent of Masson's trichrome-positive stained fibrotic lesions did not differ significantly between genotypes in WTD-fed male (Figure 5D–E) and ND-fed female mice (Figure S5B). Mac3 staining showed similar percentage of lesion areas positive for Mac3+ macrophage between groups in WTD-fed male (Figure 5F–G) and ND-fed female mice (Figure S5C), whereas a non-significant trend toward increased SM22α+ SMC content was observed in the absence of *Ilrun* (Figure S5D). Leukocytosis, including monocytosis, is a known risk factor for atherogenesis that can contribute to the imbalance of lesional leukocytes[36]. Upon WTD feeding, the ratio of blood neutrophils to lymphocytes was increased, suggesting WTD-induced systemic inflammation[37,38] that was not impacted by mouse genotype, gender, or models. Despite the difference in plasma cholesterol levels, cholesterol contents of resident peritoneal macrophages from male and female mice were similar between genotypes (Figure S6). In agreement with comparable macrophage content, blood leukocyte counts (data not shown) and distribution were overall similar between genotypes, irrespective of diet and disease model (Figure S7).

To determine whether loss of *Ilrun* decreases necrosis by altering apoptosis and efferocytosis, aortic roots were stained with TUNEL, Mac3, and DAPI using an established method[19]. Interestingly, while normalized TUNEL+ nuclei counts were comparable, the presence of *in situ* efferocytosis marker was significantly enhanced in *Ilrun*KO/*Apoe*KO relative to *Apoe*KO mice, as the ratio of free to macrophage-associated TUNEL+ apoptotic cells was markedly and significantly reduced by over 90%. Restoration of plasma lipids in *Ilrun*KO/*Apoe*KO mice led to a non-significant ~62% reduction in the ratio (p=0.0613) between genotypes (Figure 5H–I). The presence of efferocytosis markers was also measured in lesions of WTD-fed male mice on the *Ldlr*KO background. Interestingly, a significant ~75% decrease in the ratio of free to macrophage-associated TUNEL+ apoptotic cells was observed in *Ilrun*KO/*Ldlr*KO vs. *Ldlr*KO mice (Figure S8), further supporting a potential role for *Ilrun* in efferocytosis. Altogether, these results suggest *Ilrun* deficiency reduces plaque necrosis likely by enhancing efferocytosis, providing evidence of plasma lipid-independent effects of *Ilrun* that involves non-hepatic tissues.

Macrophage *Ilrun* deficiency increases MerTK protein expression and enhances *in vitro* efferocytosis

Evaluation of *in situ* efferocytosis markers suggests *Ilrun* as a potential negative regulator of efferocytosis. We therefore directly tested the effect of macrophage *Ilrun* on efferocytosis using *in vitro* assays. Resident peritoneal macrophages (PM) and bone marrow derived macrophages (BMDM) were isolated from ND-fed male mice on the *Apoe*KO background to incubate with labeled apoptotic cells (AC) and the percentage of macrophages with

engulfed AC was quantified by FACS and compared between genotypes. Interestingly, a significant ~43% and 54% increase in efferocytosis was noted for *Ilrun* deficient PM and BMDM respectively (Figure 6A–B), in support of macrophage *Ilrun* as a novel negative regulator of efferocytosis.

To explore pathways that may be impacted by *Ilrun* deletion in macrophages and mechanisms underlying increased efferocytosis in the absence of *Ilrun*, we performed RNA-seq with BMDM from ND-fed male *Apoe*KO and *Ilrun*KO/*Apoe*KO mice. Differentially expressed gene analysis revealed an overall minimal impact of *Ilrun* on macrophage transcriptome at basal level (i.e., cells from ND-fed mice), as shown in the volcano plot (Figure 6C). We also examined efferocytosis receptors with known effects in the context of atherosclerosis development[39]. Analysis of total cellular protein expression uncovered a significant increase in the abundance of MerTK, a known pivotal receptor that mediates uptake of apoptotic cells and impacting atherosclerosis[40,41]. In contrast, the protein expression of other tested receptors was comparable between genotypes (Figure 6D–E). To determine if this difference in protein expression was a result of changes in transcript expression, we tested mRNA expression of these receptors. Consistent with a minimum effect on macrophage transcriptome under this condition as suggested by RNA-seq, none of the tested efferocytosis receptor transcripts (Figure 6F), including *Mertk*, and other efferocytosis-related molecules had differential mRNA expression between groups (Figure S9). Together, these data suggest that macrophage *Ilrun* deletion enhances efferocytosis and this effect may be, at least partly, attributed to post-transcriptional regulation of MerTK expression by *Ilrun*.

Discussion

GWAS have offered the opportunity to uncover genetic loci associated with CAD and its risk factors for translating genetic findings into novel biological discoveries. Nevertheless, only a limited number of novel genetic CAD associations have been functionally validated thus far. The *ILRUN* locus is robustly associated with CAD risk[2] but remains under-studied; it is not clear that *ILRUN* is the causal gene at the locus and little is known about the function of the ILRUN protein. We addressed the genetic association of the *ILRUN* locus with CAD risk by deleting *Ilrun* in two commonly used mouse models of atherosclerosis. We found that deletion of *Ilrun* in both *Ldlr*KO and *Apoe*KO mice consistently and substantially reduced atherosclerosis lesion size, both early and advanced lesions and in both male and female mice, revealing for the first time a pro-atherogenic role for ILRUN *in vivo*. While reduced plasma cholesterol levels may have contributed to reduced atherosclerosis, our data provide evidence for pro-atherogenic actions mediated by extra-hepatic *Ilrun* (i.e., inhibition of efferocytosis by macrophage *Ilrun*), identifying two independent mechanisms that contribute to the human genetic association of the *ILRUN* locus with CAD.

We recently used whole-body *Ilrun*KO mice to show that *Ilrun* is a novel regulator of plasma lipid homeostasis that promotes hepatic lipoprotein production[14], providing mechanistic insights into the associations between human genetic variation at the 6p21 locus and plasma lipid traits[3,4]. Here, we crossed the *Ilrun*KO allele onto two atherosclerosis-prone hyperlipidemic genetic backgrounds (i.e., *Ldlr*KO and *Apoe*KO), and showed that the major

effects of *Ilrun* on plasma lipid levels persisted, supporting the notion that the lipid-lowering effect of *Ilrun* deletion is independent of the LDLR and ApoE. In the absence of *Ilrun*, plasma total cholesterol levels were decreased regardless of genetic background, diets, or the sex of the mice in this study. The reduction of plasma lipids was primarily associated with atherogenic apolipoprotein B containing lipoproteins (apoBLp), as one would predict considering highly elevated non-HDL lipoproteins in these models of disrupted apoBLp clearance[42]. Consistent with our previous finding, in this study plasma lipids of *Ilrun* deficient mice were restored to control mice levels by AAV-mediated expression of human *ILRUN* in hepatocytes, again pointing to the liver as the major site of *Ilrun* action in maintaining plasma lipid homeostasis. While the effects of *Ilrun* deficiency on plasma lipids were largely consistent across study conditions, certain genotype differences that were evident in male mice, such as HDL-C, were less obvious in female mice, particularly in mice on the *Apoe*KO background. This was possibly a result of overall relatively low lipid levels, including HDL-C, under these conditions[42] and hormonal regulations that counteracted the effect of *Ilrun*[43,44]

Beyond lipoprotein metabolism, multiple lines of evidence suggest that ILRUN also impacts atherosclerotic lesion development at the vessel wall level through additional mechanisms. First, differences in lesion size and necrosis between *Ilrun* genotypes largely persisted even when differences in plasma lipid levels were normalized by hepatocyte *ILRUN* expression. Second, efferocytosis, a classical function of macrophages and the defect of which is critical for plaque necrosis[39,45], was noticeably enhanced in macrophages lacking *Ilrun*. The presence of efferocytosis markers in lesions from *Ilrun* deficient mice was also greatly increased. Third, in support of potential tissue and cell specific roles of *Ilrun* during atherogenesis, histological and expression analyses showed ubiquitous expression of *Ilrun* in various cell types of normal arteries and developing lesions, with abundant expression in macrophages and SMC. Finally, *ILRUN* expression appears to be regulated during atherogenesis in humans[32] and emerging human genetics evidence has linked the *ILRUN* locus to lipid-independent risk factors of ASCVD, including hypertension[30,31,46].

Although the full spectrum of potential lipid-independent mechanisms in regulation of atherosclerosis by ILRUN have yet to be defined, existing results support an inhibitory role for *Ilrun* in efferocytosis: the phagocytic engulfment of dead and dying cells that involves professional phagocytes such as macrophages[45]. Indeed, results from our *in vitro* efferocytosis assays provided direct evidence of macrophage *Ilrun* as a negative regulator of efferocytosis. According to our analysis of published scRNA-seq data, *Ilrun* is highly expressed in myeloid cells, including monocytes and macrophages, among lesional immune cells. In particular, *Ilrun* is enriched in *Trem2*-high macrophages, lipid-laden macrophages in the intima and necrotic cores, that may represent a major plaque macrophage subpopulation contributing to efferocytosis[47,48] . Our previous study[14] together with published work[12] suggest that ILRUN is a regulator of protein turnover. Unlike ILRUN in the liver, the impact of *Ilrun* on macrophage transcriptome appears to be minimal at basal condition (i.e., BMDM derived from ND-fed mice) as suggested by RNA-seq analysis. This cell-type specific difference may be a result of different ILRUN target proteins. We explored the expression of known efferocytosis receptors in atherogenesis[39]. Of interest, *Ilrun* deletion specifically upregulated MerTK protein expression among tested

receptors. More importantly, no difference was observed at the transcript level for these receptors, including *Mertk*. Consistent with the concept of post-transcriptional regulation of MerTK by ILRUN, we previously showed that ILRUN interacts with ubiquitylated proteins via its UBA-like domain[14] and MerTK has been shown to have ubiquitination sites[49]. In addition, ILRUN has been implicated in cytokine production in the context of viral infection[12] and primary macrophage *Ilrun* expression is greatly induced in response to lipopolysaccharide stimulation (data not shown). As increasing evidence has linked inflammatory signaling to direct regulation of efferocytosis-related ligand expression, including induction of inactivating posttranslational modifications to “eat-me” phagocytic ligands under inflammatory conditions[45,50], it is also possible that *in vivo* ILRUN also regulates lesion inflammation to modulate molecules key to efferocytosis. The molecular mechanisms by which ILRUN impacts MertTK protein abundance and efferocytosis need to be addressed in detailed future studies.

Consistent with observations in mice, human *ILRUN* is highly expressed in normal vessels[7], including in SMC[51] and is detectable in plaque cells[32]. A role for ILRUN in SMC has not been described. Previous studies in various cancer cells have linked ILRUN to cell proliferation and invasion[9–11], and NBR1, the other protein that contains the NBR1-like domain, has been shown to interact with a microtubule associated protein MAP1B via its NBR1-like domain[52]. Moreover, common genetic variations close to *ILRUN* that associate with coronary atherosclerosis and ischemic heart disease (e.g., rs2814993-A) are also significantly associated with essential hypertension, a major risk factor for CAD in which altered vascular SMC function plays an important role[53]. Notably, these variants associate with CAD and hypertension in the same direction[30,31] (i.e, the CAD risk allele is associated with increased risk of hypertension). It is therefore of interest to explore whether ILRUN action in vascular SMC also contributes to atherogenesis, and to dissect the accumulating evidence which highlights potential distinct cell-specific roles of ILRUN.

Our study highlights the complex role of ILRUN in atherosclerosis and opens up opportunities for future endeavors. First, the relative contribution of lipid-dependent and lipid-independent factors to the observed atheroprotection in the absence of ILRUN across the spectrum of lesion progression (e.g., early and advanced lesion development) remains to be precisely defined. Second, the present study focused on the role of macrophage ILRUN in efferocytosis as an example of a lipid-independent effect on the atherosclerosis phenotype. As discussed above, ILRUN may play roles beyond regulation of efferocytosis. Exploring the impact of ILRUN on other vascular cells and immune cells relevant to atherogenesis is of great interest and an important future direction to fully understand the lipid-independent effects of ILRUN on atherosclerosis development. Lastly, further investigations are in need to uncover detailed mode of ILRUN action as a negative regulator of efferocytosis. We focused on known regulators of efferocytosis to gain mechanistic insights. Identification of protein-protein interactions critical for post-transcriptional regulation of efferocytosis regulators by ILRUN will likely provide additional novel mechanistic insights.

In summary, we investigated the effects of global loss of *Ilrun* on early and advanced atherosclerosis lesion development in male and female *Ldlr*KO and *Apoe*KO mice, finding a consistent and substantial reduction in atherosclerosis. Our studies firmly establish an

in vivo proatherogenic role for ILRUN in atherosclerosis lesion progression in mice that is attributable to both hepatic (via plasma lipid regulation) and extra-hepatic (lipid-independent) ILRUN mechanisms. This work draws a mechanistic link between ILRUN and atherosclerosis that may help explain the strong genetic association between variants at this locus and CAD. Investigation of the diverse effects of ILRUN on atherogenesis in a cell-type specific manner holds promise for a better understanding of its role and could provide insights into new approaches to the prevention and treatment of ASCVD.

Supplementary Material

Refer to Web version on PubMed Central for supplementary material.

Acknowledgments

We thank the University of Pennsylvania Histology and Gene Expression Core for assistance in tissue histology analysis, and the Preclinical Vector Core for providing gene vectors used in this study. We gratefully acknowledge Aisha Wilson, Maosen Sun, Edwige Edouard, Debra Cromley, and Amrith Rodrigues for technical assistance; Drs. Ljubica Perisic Matic, Ulf Hedin, Marie Guerraty, Jeff Billheimer, Cecilia Vitali, Joseph Park, and many former and current Rader lab members for helpful discussions. The graphic abstract was created with BioRender.com.

Sources of Funding

This work was supported by National Institutes of Health grants RC2 HL101864, R01 HL089309 (to D.J.R), American Heart Association Postdoctoral Fellowship 15POST25160019, and Career Development Award 19CDA34630032 (to X.B.), R00HL130574, R01HL151611, and the Irving Scholars Program through UL1TR001873 (to H.Z.), American Heart Association Postdoctoral Fellowship 21POST829654 (to X.W.), National Institutes of Health Fellowship F31HL149162 (to S.S.).

Abbreviations

AAV	Adeno-Associated Virus
ASCVD	Atherosclerotic Cardiovascular Disease
***Apoe*KO**	Apolipoprotein E Knockout
CAD	Coronary Artery Disease
DKO	Double Knockout
EC	Endothelial Cell
FPLC	Fast Protein Liquid Chromatography
GWAS	Genome Wide Association Studies
HDL-C	High-density Lipoprotein-Cholesterol
ILRUN	Inflammation and Lipid Regulator with UBA-like and NBR1-like domains
***Ldlr*KO**	Low-density Lipoprotein Receptor Knockout
NBR1	Next to BRCA1 Gene 1 Protein

ND	Normal Laboratory Diet
PL	Phospholipid
SKO	Single Knockout
SMC	Smooth Muscle Cell
TC	Total Cholesterol
TG	Triglycerides
UBA	Ubiquitin Associated Domain
VLDL	Very-low Density Lipoprotein
WTD	Western Type Diet

References

1. Libby P, Buring JE, Badimon L, Hansson GK, Deanfield J, Bittencourt MS, Tokgozoglu L, Lewis EF. Atherosclerosis. Nat Rev Dis Primers. 2019;5:56. doi: 10.1038/s41572-019-0106-z [PubMed: 31420554]
2. van der Harst P, Verweij N. Identification of 64 Novel Genetic Loci Provides an Expanded View on the Genetic Architecture of Coronary Artery Disease. Circ Res. 2018;122:433–443. doi: 10.1161/CIRCRESAHA.117.312086 [PubMed: 29212778]
3. Teslovich TM, Musunuru K, Smith AV, et al. Biological, clinical and population relevance of 95 loci for blood lipids. Nature. 2010;466:707–713. doi: 10.1038/nature09270 [PubMed: 20686565]
4. Willer CJ, Schmidt EM, Sengupta S, et al. Discovery and refinement of loci associated with lipid levels. Nat Genet. 2013;45:1274–1283. doi: 10.1038/ng.2797 [PubMed: 24097068]
5. Klarin D, Damrauer SM, Cho K, et al. Genetics of blood lipids among ~300,000 multi-ethnic participants of the Million Veteran Program. Nature genetics. 2018. doi: 10.1038/s41588-018-0222-9
6. Lu X, Peloso GM, Liu DJ, et al. Exome chip meta-analysis identifies novel loci and East Asian-specific coding variants that contribute to lipid levels and coronary artery disease. Nature genetics. 2017;49:1722–1730. doi: 10.1038/ng.3978 [PubMed: 29083407]
7. Consortium GT, Laboratory DA, Coordinating Center -Analysis Working G, et al. Genetic effects on gene expression across human tissues. Nature. 2017;550:204–213. doi: 10.1038/nature24277 [PubMed: 29022597]
8. Marchler-Bauer A, Derbyshire MK, Gonzales NR, et al. CDD: NCBI's conserved domain database. Nucleic Acids Res. 2015;43:D222–226. doi: 10.1093/nar/gku1221 [PubMed: 25414356]
9. Zhang X, Miao Y, Yu X, Zhang Y, Jiang G, Liu Y, Yu J, Han Q, Zhao H, Wang E. C6orf106 enhances NSCLC cell invasion by upregulating vimentin, and downregulating E-cadherin and P120ctn. Tumour Biol. 2015;36:5979–5985. doi: 10.1007/s13277-015-3274-9 [PubMed: 25736925]
10. Jiang G, Zhang X, Zhang Y, Wang L, Fan C, Xu H, Miao Y, Wang E. A novel biomarker C6orf106 promotes the malignant progression of breast cancer. Tumour Biol. 2015;36:7881–7889. doi: 10.1007/s13277-015-3500-5 [PubMed: 25953261]
11. Li X, Dong M, Zhou J, Zhu D, Zhao J, Sheng W. C6orf106 accelerates pancreatic cancer cell invasion and proliferation via activating ERK signaling pathway. Mol Cell Biochem. 2019;454:87–95. doi: 10.1007/s11010-018-3455-0 [PubMed: 30311108]
12. Ambrose RL, Liu YC, Adams TE, Bean AGD, Stewart CR. C6orf106 is a novel inhibitor of the interferon-regulatory factor 3-dependent innate antiviral response. J Biol Chem. 2018;293:10561–10573. doi: 10.1074/jbc.RA117.001491 [PubMed: 29802199]
13. Ambrose RL, Brice AM, Caputo AT, Alexander MR, Tribolet L, Liu YC, Adams TE, Bean AGD, Stewart CR. Molecular characterisation of ILRUN, a novel inhibitor of proinflammatory and

antimicrobial cytokines. Heliyon. 2020;6:e04115. doi: 10.1016/j.heliyon.2020.e04115 [PubMed: 32518853]

14. Bi X, Kuwano T, Lee PC, Millar JS, Li L, Shen Y, Soccio RE, Hand NJ, Rader DJ. ILRUN, a Human Plasma Lipid GWAS Locus, Regulates Lipoprotein Metabolism in Mice. Circ Res. 2020;127:1347–1361. doi: 10.1161/CIRCRESAHA.120.317175 [PubMed: 32912065]
15. Consortium CAD, Deloukas P, Kanoni S, et al. Large-scale association analysis identifies new risk loci for coronary artery disease. Nat Genet. 2013;45:25–33. doi: 10.1038/ng.2480 [PubMed: 23202125]
16. Nikpay M, Goel A, Won HH, et al. A comprehensive 1,000 Genomes-based genome-wide association meta-analysis of coronary artery disease. Nat Genet. 2015;47:1121–1130. doi: 10.1038/ng.3396 [PubMed: 26343387]
17. Papatheodorou I, Moreno P, Manning J, et al. Expression Atlas update: from tissues to single cells. Nucleic Acids Res. 2020;48:D77–D83. doi: 10.1093/nar/gkz947 [PubMed: 31665515]
18. Lukowski SW, Patel J, Andersen SB, Sim SL, Wong HY, Tay J, Winkler I, Powell JE, Khosrotehrani K. Single-Cell Transcriptional Profiling of Aortic Endothelium Identifies a Hierarchy from Endovascular Progenitors to Differentiated Cells. Cell Rep. 2019;27:2748–2758 e2743. doi: 10.1016/j.celrep.2019.04.102 [PubMed: 31141696]
19. Doran AC, Ozcan L, Cai B, Zheng Z, Fredman G, Rymond CC, Dorweiler B, Sluimer JC, Hsieh J, Kuriakose G, Tall AR, Tabas I. CAMKIIgamma suppresses an efferocytosis pathway in macrophages and promotes atherosclerotic plaque necrosis. J Clin Invest. 2017;127:4075–4089. doi: 10.1172/JCI94735 [PubMed: 28972541]
20. Martinez J, Cunha LD, Park S, Yang M, Lu Q, Orchard R, Li QZ, Yan M, Janke L, Guy C, Linkermann A, Virgin HW, Green DR. Corrigendum: Noncanonical autophagy inhibits the autoinflammatory, lupus-like response to dying cells. Nature. 2016;539:124. doi: 10.1038/nature19837 [PubMed: 27680703]
21. Moon H, Min C, Kim G, Kim D, Kim K, Lee SA, Moon B, Yang S, Lee J, Yang SJ, Cho SK, Lee G, Lee CS, Park CS, Park D. Crbn modulates calcium influx by regulating Orai1 during efferocytosis. Nat Commun. 2020;11:5489. doi: 10.1038/s41467-020-19272-0 [PubMed: 33127885]
22. Patro R, Duggal G, Love MI, Irizarry RA, Kingsford C. Salmon provides fast and bias-aware quantification of transcript expression. Nat Methods. 2017;14:417–419. doi: 10.1038/nmeth.4197 [PubMed: 28263959]
23. Soneson C, Love MI, Robinson MD. Differential analyses for RNA-seq: transcript-level estimates improve gene-level inferences. F1000Res. 2015;4:1521. doi: 10.12688/f1000research.7563.2 [PubMed: 26925227]
24. Love MI, Huber W, Anders S. Moderated estimation of fold change and dispersion for RNA-seq data with DESeq2. Genome Biol. 2014;15:550. doi: 10.1186/s13059-014-0550-8 [PubMed: 25516281]
25. Bi X, Zhu X, Gao C, Shewale S, Cao Q, Liu M, Boudyguina E, Gebre AK, Wilson MD, Brown AL, Parks JS. Myeloid cell-specific ATP-binding cassette transporter A1 deletion has minimal impact on atherogenesis in atherogenic diet-fed low-density lipoprotein receptor knockout mice. Arterioscler Thromb Vasc Biol. 2014;34:1888–1899. doi: 10.1161/ATVBAHA.114.303791 [PubMed: 24833800]
26. Hao Y, Hao S, Andersen-Nissen E, et al. Integrated analysis of multimodal single-cell data. Cell. 2021;184:3573–3587.e3529. doi: 10.1016/j.cell.2021.04.048 [PubMed: 34062119]
27. Cochain C, Vafadarnejad E, Arampatzi P, Pelisek J, Winkels H, Ley K, Wolf D, Saliba AE, Zernecke A. Single-Cell RNA-Seq Reveals the Transcriptional Landscape and Heterogeneity of Aortic Macrophages in Murine Atherosclerosis. Circ Res. 2018;122:1661–1674. doi: 10.1161/CIRCRESAHA.117.312509 [PubMed: 29545365]
28. Zernecke A, Winkels H, Cochain C, et al. Meta-Analysis of Leukocyte Diversity in Atherosclerotic Mouse Aortas. Circ Res. 2020;127:402–426. doi: 10.1161/CIRCRESAHA.120.316903 [PubMed: 32673538]
29. Villani AC, Satija R, Reynolds G, et al. Single-cell RNA-seq reveals new types of human blood dendritic cells, monocytes, and progenitors. Science. 2017;356. doi: 10.1126/science.aah4573

30. Bycroft C, Freeman C, Petkova D, et al. The UK Biobank resource with deep phenotyping and genomic data. Nature. 2018;562:203–209. doi: 10.1038/s41586-018-0579-z [PubMed: 30305743]
31. Gagliano Taliun SA, VandeHaar P, Boughton AP, Welch RP, Taliun D, Schmidt EM, Zhou W, Nielsen JB, Willer CJ, Lee S, Fritsche LG, Boehnke M, Abecasis GR. Exploring and visualizing large-scale genetic associations by using PheWeb. Nat Genet. 2020;52:550–552. doi: 10.1038/s41588-020-0622-5 [PubMed: 32504056]
32. Sulkava M, Raitoharju E, Levula M, et al. Differentially expressed genes and canonical pathway expression in human atherosclerotic plaques - Tampere Vascular Study. Sci Rep. 2017;7:41483. doi: 10.1038/srep41483 [PubMed: 28128285]
33. Folkersen L, Persson J, Ekstrand J, Agardh HE, Hansson GK, Gabrielsen A, Hedin U, Paulsson-Berne G. Prediction of ischemic events on the basis of transcriptomic and genomic profiling in patients undergoing carotid endarterectomy. Mol Med. 2012;18:669–675. doi: 10.2119/molmed.2011.00479 [PubMed: 22371308]
34. Lee K, Santibanez-Koref M, Polvikoski T, Birchall D, Mendelow AD, Keavney B. Increased expression of fatty acid binding protein 4 and leptin in resident macrophages characterises atherosclerotic plaque rupture. Atherosclerosis. 2013;226:74–81. doi: 10.1016/j.atherosclerosis.2012.09.037 [PubMed: 23122912]
35. Daugherty A, Tall AR, Daemen M, Falk E, Fisher EA, Garcia-Cardena G, Lusis AJ, Owens AP 3rd, Rosenfeld ME, Virmani R. Recommendation on Design, Execution, and Reporting of Animal Atherosclerosis Studies: A Scientific Statement From the American Heart Association. Arterioscler Thromb Vasc Biol. 2017;37:e131–e157. doi: 10.1161/ATV.0000000000000062 [PubMed: 28729366]
36. Swirski FK, Nahrendorf M. Leukocyte behavior in atherosclerosis, myocardial infarction, and heart failure. Science. 2013;339:161–166. doi: 10.1126/science.1230719 [PubMed: 23307733]
37. Lee YR, Joo HK, Lee EO, Park MS, Cho HS, Kim S, Jin H, Jeong JO, Kim CS, Jeon BH. Plasma APE1/Ref-1 Correlates with Atherosclerotic Inflammation in ApoE. Biomedicines. 2020;8. doi: 10.3390/biomedicines8090366
38. Chung D, Lee KO, Choi JW, Kim NK, Kim OJ, Kim SH, Oh SH, Kim WC. Blood Neutrophil/Lymphocyte Ratio Is Associated With Cerebral Large-Artery Atherosclerosis but Not With Cerebral Small-Vessel Disease. Front Neurol. 2020;11:1022. doi: 10.3389/fneur.2020.01022 [PubMed: 33013672]
39. Yurdagul A Jr., Doran AC, Cai B, Fredman G, Tabas IA. Mechanisms and Consequences of Defective Efferocytosis in Atherosclerosis. Front Cardiovasc Med. 2017;4:86. doi: 10.3389/fcvm.2017.00086 [PubMed: 29379788]
40. Thorp E, Cui D, Schrijvers DM, Kuriakose G, Tabas I. Mertk receptor mutation reduces efferocytosis efficiency and promotes apoptotic cell accumulation and plaque necrosis in atherosclerotic lesions of apoe−/− mice. Arterioscler Thromb Vasc Biol. 2008;28:1421–1428. doi: 10.1161/ATVBAHA.108.167197 [PubMed: 18451332]
41. Cai B, Thorp EB, Doran AC, Sansbury BE, Daemen MJ, Dorweiler B, Spite M, Fredman G, Tabas I. MerTK receptor cleavage promotes plaque necrosis and defective resolution in atherosclerosis. J Clin Invest. 2017;127:564–568. doi: 10.1172/JCI90520 [PubMed: 28067670]
42. Getz GS, Reardon CA. Do the Apoe−/− and Ldlr−/− Mice Yield the Same Insight on Atherogenesis? Arterioscler Thromb Vasc Biol. 2016;36:1734–1741. doi: 10.1161/ATVBAHA.116.306874 [PubMed: 27386935]
43. Yoon M, Jeong S, Nicol CJ, Lee H, Han M, Kim JJ, Seo YJ, Ryu C, Oh GT. Fenofibrate regulates obesity and lipid metabolism with sexual dimorphism. Exp Mol Med. 2002;34:481–488. doi: 10.1038/emm.2002.67 [PubMed: 12526091]
44. Yoon M The role of PPARalpha in lipid metabolism and obesity: focusing on the effects of estrogen on PPARalpha actions. Pharmacol Res. 2009;60:151–159. doi: 10.1016/j.phrs.2009.02.004 [PubMed: 19646654]
45. Kojima Y, Weissman IL, Leeper NJ. The Role of Efferocytosis in Atherosclerosis. Circulation. 2017;135:476–489. doi: 10.1161/CIRCULATIONAHA.116.025684 [PubMed: 28137963]

46. Bi W, Fritsche LG, Mukherjee B, Kim S, Lee S. A Fast and Accurate Method for Genome-Wide Time-to-Event Data Analysis and Its Application to UK Biobank. Am J Hum Genet. 2020;107:222–233. doi: 10.1016/j.ajhg.2020.06.003 [PubMed: 32589924]

47. Willemsen L, de Winther MP. Macrophage subsets in atherosclerosis as defined by single-cell technologies. J Pathol. 2020;250:705–714. doi: 10.1002/path.5392 [PubMed: 32003464]

48. Kim K, Shim D, Lee JS, et al. Transcriptome Analysis Reveals Nonfoamy Rather Than Foamy Plaque Macrophages Are Proinflammatory in Atherosclerotic Murine Models. Circ Res. 2018;123:1127–1142. doi: 10.1161/CIRCRESAHA.118.312804 [PubMed: 30359200]

49. Chen T, Zhou T, He B, Yu H, Guo X, Song X, Sha J. mUbiSiDa: a comprehensive database for protein ubiquitination sites in mammals. PLoS One. 2014;9:e85744. doi: 10.1371/journal.pone.0085744 [PubMed: 24465676]

50. Tabas I Macrophage death and defective inflammation resolution in atherosclerosis. Nat Rev Immunol. 2010;10:36–46. doi: 10.1038/nri2675 [PubMed: 19960040]

51. Wang D, Eraslan B, Wieland T, et al. A deep proteome and transcriptome abundance atlas of 29 healthy human tissues. Mol Syst Biol. 2019;15:e8503. doi: 10.15252/msb.20188503 [PubMed: 30777892]

52. Marchbank K, Waters S, Roberts RG, Solomon E, Whitehouse CA. MAP1B Interaction with the FW Domain of the Autophagic Receptor Nbr1 Facilitates Its Association to the Microtubule Network. Int J Cell Biol. 2012;2012:208014. doi: 10.1155/2012/208014 [PubMed: 22654911]

53. Touyz RM, Alves-Lopes R, Rios FJ, Camargo LL, Anagnostopoulou A, Arner A, Montezano AC. Vascular smooth muscle contraction in hypertension. Cardiovasc Res. 2018;114:529–539. doi: 10.1093/cvr/cvy023 [PubMed: 29394331]

Highlights

- *Ilrun is* a novel regulator of atherosclerosis development.
- *Ilrun* deficiency in the liver reduces plasma cholesterol levels and attenuates atherogenesis.
- *Ilrun* deficiency in extra-hepatic tissues is atheroprotective via lipid-independent mechanisms.
- *Ilrun* deficiency in macrophages enhances efferocytosis.

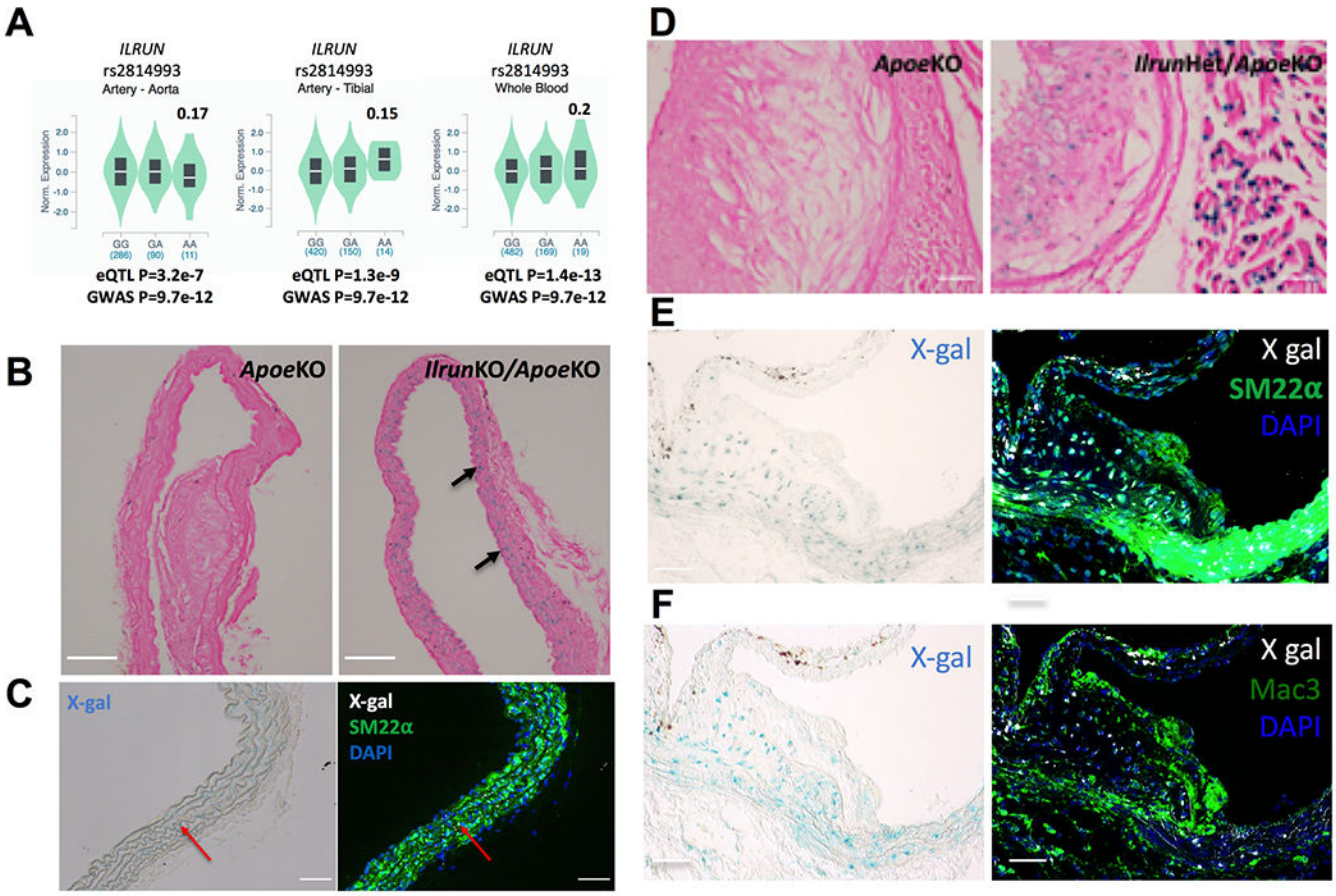

Figure 1. ILRUN expression in CAD relevant tissues.

A, eQTL results from the Genotype Tissue Expression project for rs2814993. Violin plots of normalized expression of *ILRUN* by genotype in aorta, tibial artery, and whole blood. Numbers indicate normalized effect size that is computed as the effect of the alternative allele (A) relative to the reference allele (G). **B**, Brachiocephalic artery sections from ND-fed male mice stained with X-gal and light eosin. **C**, Thoracic aorta sections from female mice stained with X-gal, SM22α, and DAPI. **D**, Aortic root sections from ND-fed male mice stained with X-gal and light eosin. Aortic root sections from ND-fed *Ilrun*KO/*Apoe*KO male mice were stained with X-gal, DAPI, and SM22α (**E**) or Mac3 (**F**). Scale bars represent 100μm in B-C and 50μm in D-F. Arrows in B-C point to representative X-gal positive signals.

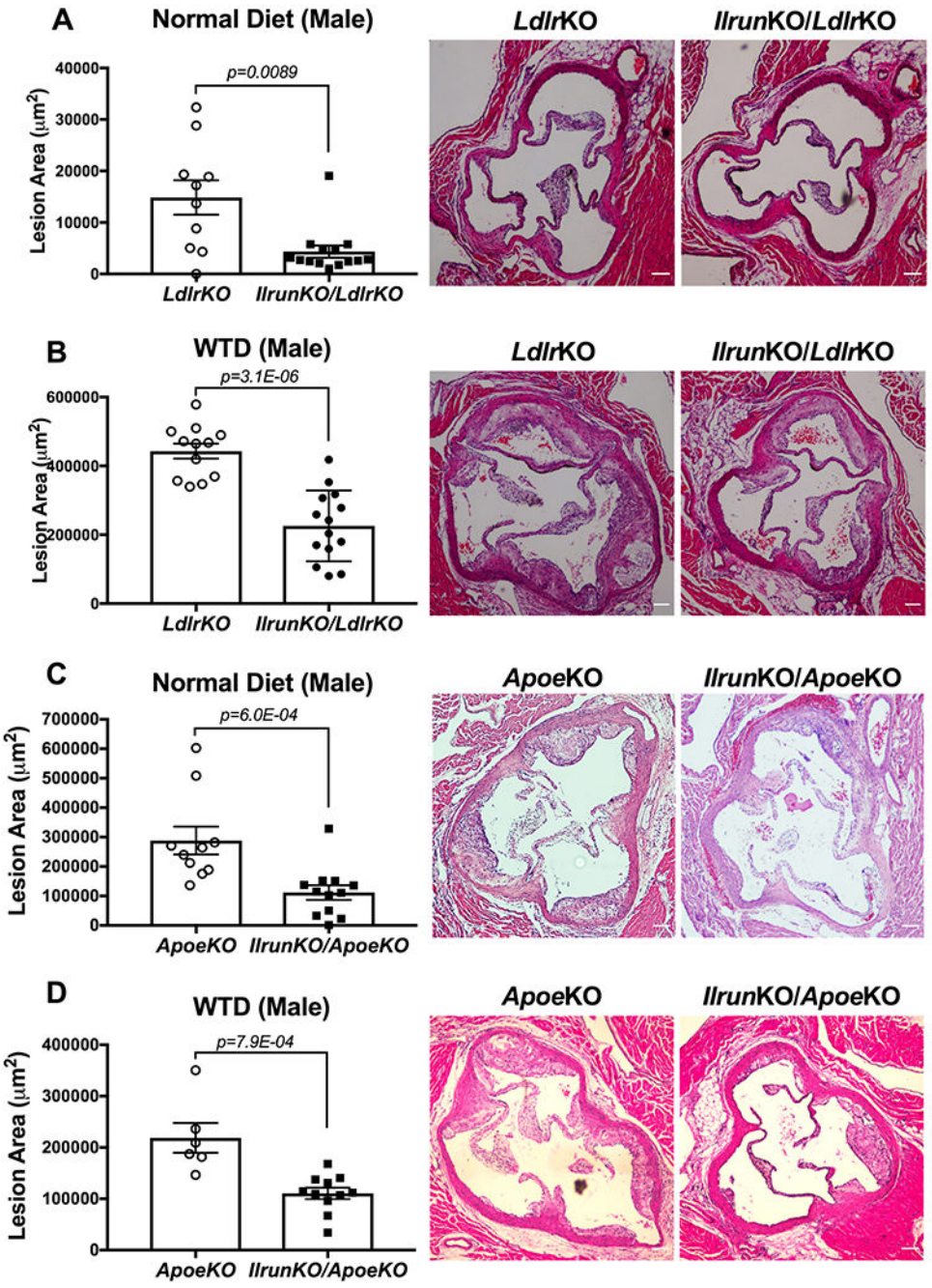

Figure 2. *Ilrun* deficiency attenuates atherosclerosis in *Ldlr*KO and *Apoe*KO mice.

Aortic roots from male mice on the *Ldlr*KO background fed with ND for 24 weeks (**A**) or WTD for 16 weeks (**B**) were used for lesion area quantification. Aortic root lesion areas from male mice on the *Apoe*KO background fed with ND till 28 weeks of age (**C**) or WTD for 10 weeks (**D**) were determined. Representative images of sections stained with H&E are shown on the right. Scale bars represent 100μm. Data are shown as the mean ± SEM. Results in A and C were compared with Mann-Whitney test. Results in B and D were compared with Student's t test. P values indicate comparisons between genotypes.

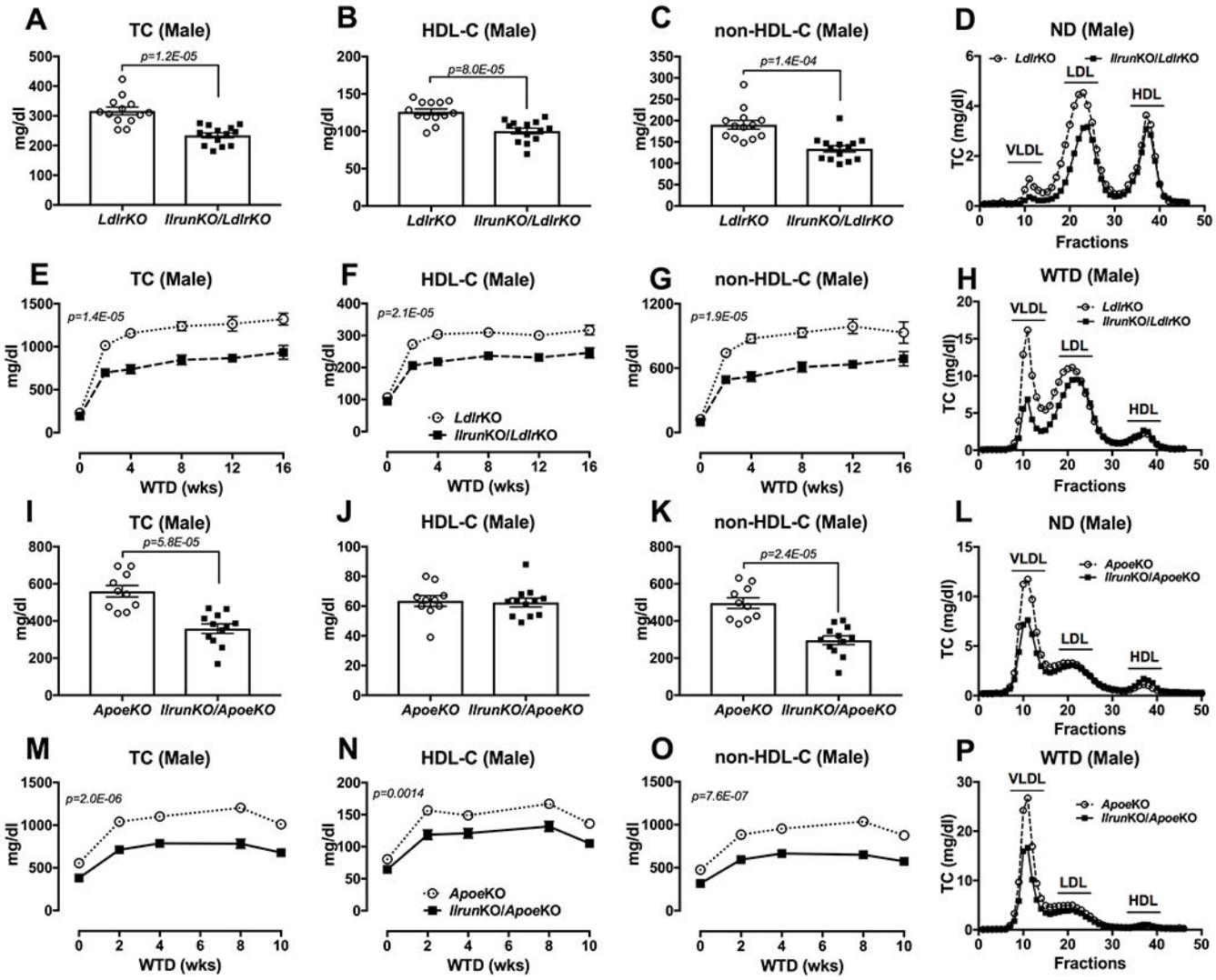

Figure 3. *Ilrun* deletion lowers plasma cholesterol levels in *Ldlr*KO and *Apoe*KO mice.

Four-hour fasted plasma from ND-fed male *Ldlr*KO and *Ilrun*KO/*Ldlr*KO mice was collected; plasma (**A**) TC and (**B**) HDL-C levels were measured. **C**, Non–HDL-C was calculated by subtracting HDL-C from TC. **D**, FPLC fractionation of pooled plasma for TC analysis from each genotype. Mice were switched from ND to WTD for 16 weeks. Time course plasma (**E**)TC, (**F**) HCL-C, and (**G**) non–HDL-C were determined. **H**, Pooled plasma from these mice were fractionated by FPLC. For mice on the *Apoe*KO background, plasma (**I**) TC and (**J**) HDL-C levels of ND-fed male mice were measured using four-hour fasted plasma. **K**, Non–HDL-C was calculated by subtracting HDL-C from TC. **L**, FPLC fractionation of pooled plasma from ND-fed mice followed by TC enzymatic assays. Mice were switched from ND to WTD for 10 weeks. Plasma (**M**) TC, (**N**) HCL-C, and (**O**) non–HDL-C were determined periodically. **P**, Pooled plasma from WTD-fed mice were fractionated by FPLC for TC analysis. Data are shown as the mean ± SEM. Results in A-C and I-K were compared with Student's t test. Results in E-G and M-O were compared with two-way ANOVA. P values indicate comparisons between genotypes.

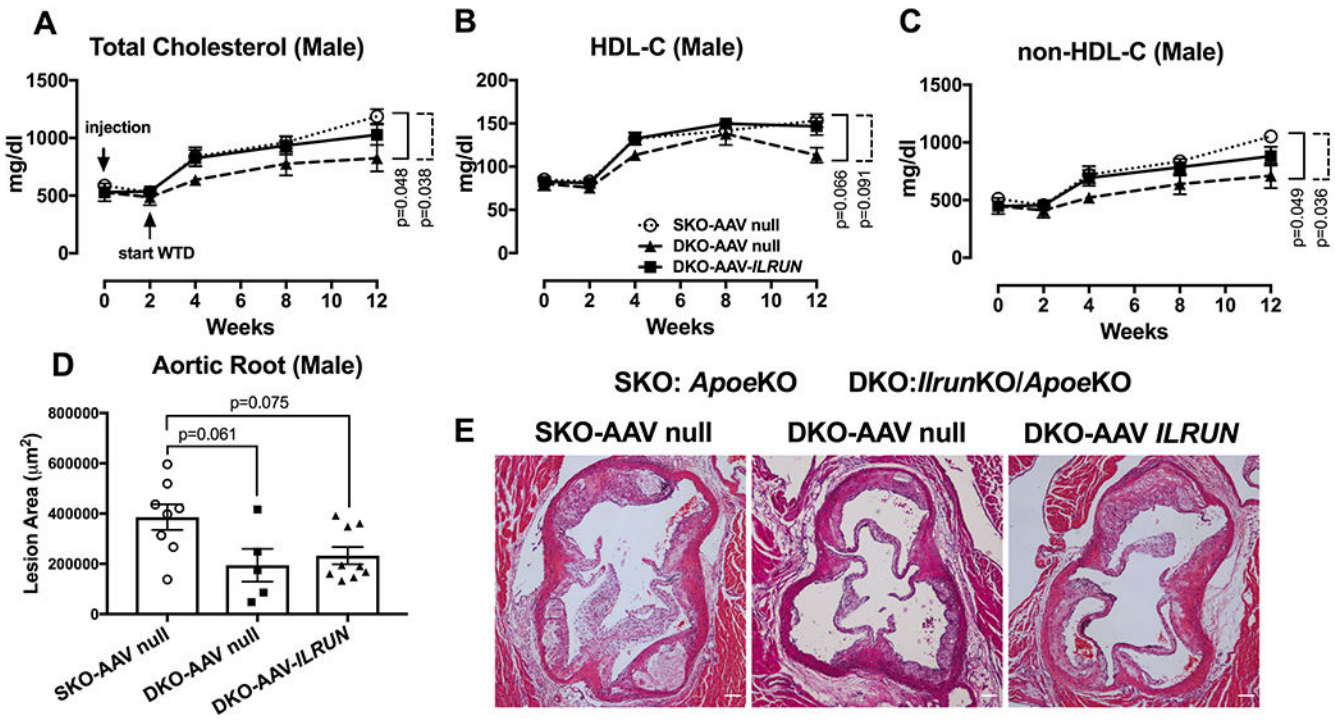

Figure 4. Hepatic *ILRUN* reconstitution in *Ilrun* deficient *Apoe*KO male mice restores plasma lipids but lesion size remains reduced.

ND-fed male mice were i.p. injected with AAV-null or AAV-*ILRUN*. Two weeks after AAV injection, mice were switched from ND to WTD for 10 weeks and sacrificed at ~23 weeks of age. Plasma lipid levels were monitored before (week 0), 2, 4, 8 and 12 weeks after AAV injection. Plasma TC (**A**) and HDL-C (**B**) levels were measured. **C**, Non–HDL-C was calculated by subtracting HDL-C from TC. Aortic root lesion areas were measured (**D**) and representative H&E stained images are shown (**E**). SKO indicates *Apoe*KO and DKO indicates *Ilrun*KO/*Apoe*KO. Scale bars represent 100μm. Data are shown as the mean ± SEM. Results in A-C were compared with two-way ANOVA with Tukey's multiple comparisons test. Results in D were compared with Kruskal-Wallis test with Dunn's multiple comparisons test for comparison with SKO-AAVnull. P values represent comparisons between indicated groups.

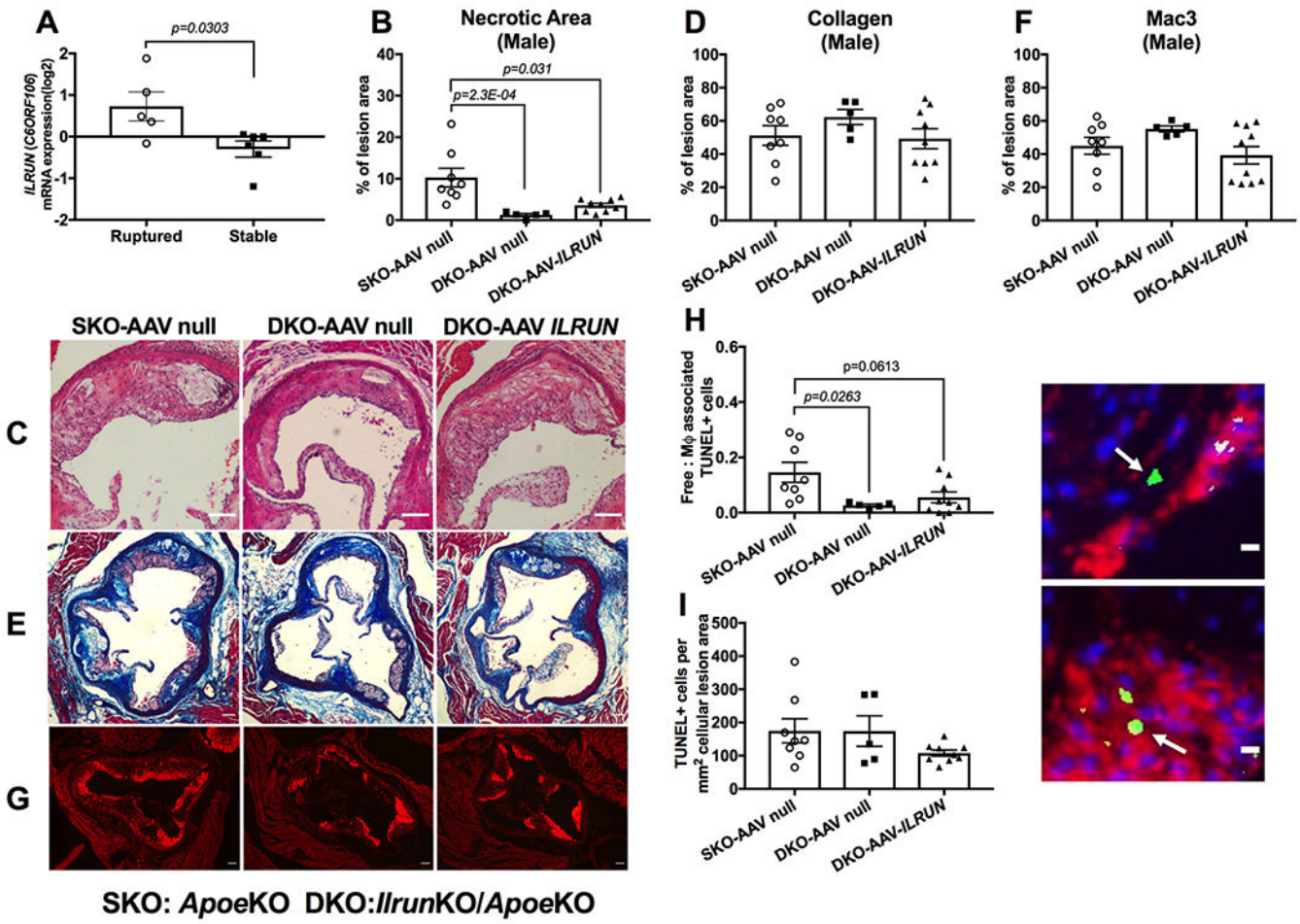

Figure 5. *Ilrun* deficiency in *Apoe*KO mice increases the presence of efferocytosis markers and reduces plaque necrosis.

A, *ILRUN* expression in laser-micro-dissected macrophages from ruptured vs. stable plaques. Aortic roots from the hepatic *ILRUN* reconstitution study (male mice on WTD sacrificed at ~23 weeks of age) were stained and analyzed for necrotic area (**B-C**), collagen content (**D-E**), macrophage content (**F-G**), efferocytosis (**H**) and apoptotic cells (**I**). SKO indicates *Apoe*KO and DKO indicates *Ilrun*KO/*Apoe*KO. Representative images next to H & I (right) indicate free (top) and macrophage associated TUNEL+ nuclei (bottom) respectively. Scale bars represent 100μm in C,E,G and 10μm in H. Data are shown as the mean ± SEM. Results in A were compared with Mann-Whitney test. Results in B, D, F, H, and I were compared with Kruscal-Wallis test with Dunn's multiple comparisons test for comparison with SKO-AAVnull. P values represent comparisons between indicated groups.

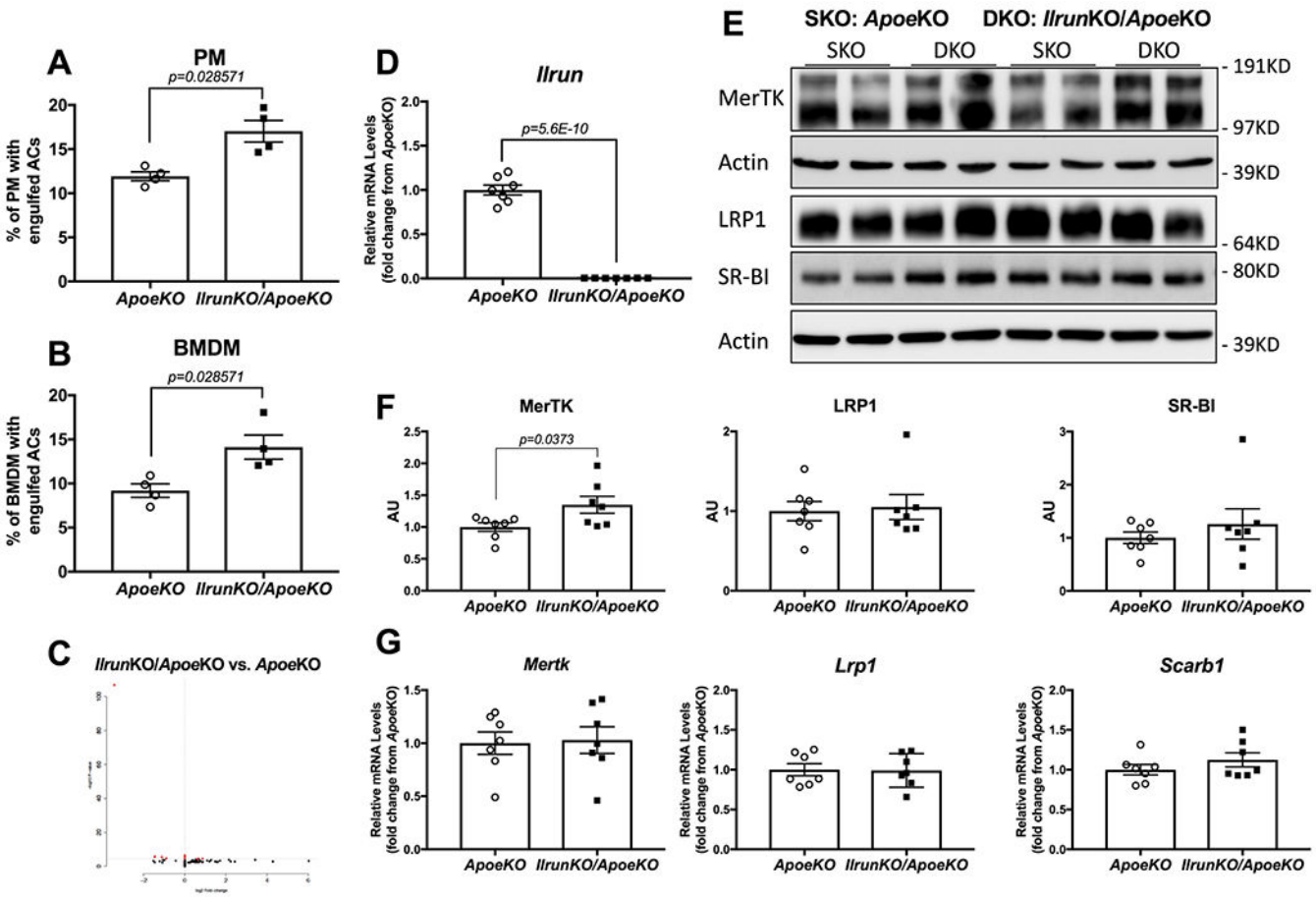

Figure 6. *Ilrun* deficiency in macrophages increases MerTK protein expression and enhances *in vitro* efferocytosis.

Resident peritoneal macrophages (**A**) and bone marrow derived macrophages (**B**) from ND-fed male mice on the *Apoe*KO background were used for in vitro efferocytosis assays. Percentage of macrophages with engulfed apoptotic cells are presented. **C**. The volcano plot of BMDM RNA-seq results comparing *Ilrun*KO/*Apoe*KO vs. *Apoe*KO macrophages from ND-fed male mice. **D**. *Ilrun* mRNA expression in BMDM of ND-fed male mice. Total protein expression of known efferocytosis receptors and loading control (Actin) were compared between BMDM samples from *Apoe*KO and *Ilrun*KO/*Apoe*KO male mice. Representative images (**E**) and quantitation of protein abundance (**F**) are shown. **G**. Expression of efferocytosis receptor mRNA in BMDM was measured with samples derived from the same mice tested in E-F. Data are shown as the mean ± SEM. Results in A and B were compared with Mann-Whitney test. Results in E-G were compared with Student's t test. P values represent comparisons between indicated groups.